Available online at www.sciencedirect.com
SCIENCE DIRECT
ELSEVIER
Ocean Engineering 32 (2005) 783–801
OCEAN ENGINEERING
www.elsevier.com/locate/oceaneng

Numerical and experimental study on hydrodynamic interaction of side-by-side moored multiple vessels

S.Y. Hong[a,*], J.H. Kim[a], S.K. Cho[a], Y.R. Choi[b], Y.S. Kim[c]

[a]*Korea Research Institute of Ships and Ocean Engineering, KORDI, P.O. Box 23, Yusong, Daejeon 305-600, Republic of South Korea*
[b]*Ulsan University, Muger 2-dong, Ulsan 680-749, Republic of South Korea*
[c]*Daewoo Shipbuilding and Marine Engineering Co., Ltd, 1-Aju-dong, Koje, Kyungnam 656-714, Republic of South Korea*

Available online 8 December 2004

Abstract

This paper aims to investigate the basic interaction characteristics of side-by-side moored vessels both numerically and experimentally. A higher-order boundary element method (HOBEM) combined with generalized mode approach is applied to analysis of motion and drift force of side-by-side moored multiple vessels (LNG FPSO, LNGC and shuttle tankers). Model tests were carried out for the same floating bodies investigated in the numerical study in regular and irregular waves. Global and local motion responses and drift forces of three vessels are compared with those of calculations. Discussions is highlighted on applicability of numerical method to prediction of sophisticated multi-body interaction problem of which motion behavior is very important to analysis of mooring dynamics of deep sea floating bodies.

Keywords: Hydrodynamic interaction; Side-by-side mooring; Higher-order boundary element method (HOBEM); Motion response; Drift force; Helmholtz resonance

1. Introduction

One of noticeable features of deep sea moored vessel is a need of multi-body operation such as offloading of FPSO–shuttle tanker system. Side-by-side offloading operation

* Corresponding author. Tel.: +82 42 868 7521; fax: +82 42 868 7519.
E-mail address: sayhong@kriso.re.kr (S.Y. Hong).

0029-8018/$ - see front matter © 2004 Elsevier Ltd. All rights reserved.
doi:10.1016/j.oceaneng.2004.10.003

Nomenclature

A	amplitude of incident wave
a_{ij}	added mass of ith mode due to jth mode motion
B	breadth
C_{ij}	hydrostatic restoring coefficient matrix
$c(x)$	solid angle
F_{DWx}, F_{Dwy}	longitudinal and lateral wave drift forces
F_j	external force vector
FP, Mid, AP	forward perpendicular, mid ship and after perpendicular, respectively
G,G_{n}	wave Green function and its normal derivative
GM	transverse metacentric height
$H_{1/3}$	significant wave height
K	wave number
KG	height of center of gravity from the bottom of the structure
k_{ij}	mooring spring constant
k_{xx},k_{yy},k_{zz}	radius of gyration of roll, pitch and yaw, respectively
LCG	longitudinal center of gravity
L_{pp}	length between perpendiculars
NB	number of bodies
M_{ij}	mass matrix
N_l	directional cosine of lth mode motion of a single body
n_j	generalized directional cosine of jth mode motion of multiple body
R_{ij}	retardation function matrix
RBM	relative bow motion ≡ relative wave
S_j	mean wetted surface of jth body
T_{p}	modal period, peak period of the wave spectrum
x_j	motion vector
Δ	displacement in ton
ϕ,ϕ_{n}	total velocity potential and its normal derivative
ϕ_{I}	incident wave potential
ϕ_j	radiation potential due to jth mode motion
ϕ_{s}	scattering potential
η_j	complex amplitude of jth mode motion
ζ	wave elevation of an irregular sea

recently devised for LNG FPSO has been paid attention, because it requires more accurate analysis of hydrodynamic interactions between closely side-by-side moored LNG FPSO and LNGC(LNG Carrier) than tandem moored vessels.

For the problems of hydrodynamic interactions between multiple bodies, a number of remarkable works has been found; Ohkusu (1974); Kodan (1984); Fang and Kim (1986) applied strip theory to analysis of hydrodynamic interaction problem between two vessels positioned in parallel. Van Oortmerssen (1979) and Loken (1981) used

the three-dimensional linear diffraction theory to solve similar problems. Fang and Chen (2001, 2002) used three-dimensional source distribution method to predict wave forces and motions of two bodies. Choi and Hong (2002) applied HOBEM to analysis of hydrodynamic interactions of multi-body system.

Huijsmans et al. (2001) found that numerical exaggeration occurred due to numerical inaccuracy in constant panel method when the distance between two vessels is very close. They imposed rigid wall condition on the free surface region between two vessels to suppress such numerical problem. Buchner et al. (2001) developed numerical simulation model for hydrodynamic response of LNG–FPSO with alongside moored LNGC in time domain. Inoue and Islam (2001) reported abnormal sensitivity to roll motion in calculation of drift force in side-by-side moored vessels. While, Hong et al. (1999) showed HOBEM provide more accurate results for analysis of hydrodynamic interaction between multiple bodies with numerical and experimental examples.

It is expected that chance of multiple body operation will be increasing more and more as water depth is becoming deeper and deeper, and the number of floating bodies in simultaneous operation will be also growing accordingly. So, it is worth investigating reliability of numerical analysis method for hydrodynamic interaction of multiple bodies directly affecting mooring performance in waves.

In this paper, basic interaction characteristics of side-by-side moored vessels are investigated both numerically and experimentally. A higher-order boundary element method combined with generalized mode approach is applied to analysis of motion and drift force of side-by-side moored vessels (LNG FPSO, LNGC and shuttle tankers). Model tests were carried out for the same bodies in regular and irregular waves. Numerical results are compared with experiments for global and local motion responses and drift forces. Applicability of numerical method to prediction of sophisticated multi-body interaction problem is discussed, of which motion behavior is very important to analysis of mooring dynamics of deep sea floating bodies.

2. Numerical analysis

It is effective to adopt generalized mode concept to solving multi-body hydrodynamic interaction problems. For a multi-body system of NB body units, the concept of generalized mode leads to $6\times$NB degrees of freedom assuming each body behaves as a rigid body (Lee & Choi, 1998).

Hydrodynamic interaction characteristics of side-by-side moored vessels are very similar to that of a vessel moored to quay. Hong et al. (2002) showed use of higher order boundary element method can suppress numerical exaggeration encountered when conventional constant panel method (CPM) is used. Huijsmans et al. (2001) imposed an artificial condition on the free surface between two side-by-side moored vessels to suppress unrealistic numerical overstatement. HOBEM is known to provide more accurate results than CPM thanks to its capability of representing abrupt change of body geometry by using higher-order interpolation functions (Liu et al., 1990). In the present study, 9-node bi-quadratic HOBEM is applied to analysis of hydrodynamic interactions between side-by-side moored vessels.

2.1. Frequency-domain analysis

Velocity potential is introduced and boundary value problem is formulated. Based on the perturbation method for small amplitude waves, the velocity potential and other physical quantities are expanded with respect to the mean position. The first-order boundary value problem is well known, for example in Newman (1977), which can be decomposed into radiation and diffraction problem.

Normally, 6 degree of freedom is used to describe the motions of a single rigid body. For a multi-body system composed of NB units, application of generalized mode approach leads to 6×NB degrees of freedom (Lee & Choi, 1998).

The radiation boundary condition is expressed as below;

$$\frac{\partial \phi_j}{\partial n} = -i\omega n_j, \text{ on } \sum_{k=1}^{\mathrm{NB}} S_k, (j = 1, \ldots 6 \times \mathrm{NB}) \tag{1}$$

In above equation, j is counted from 1 to 6×NB and the generalized directional cosine, n_j is expressed as the directional cosine, N_l, of rigid body motions for each body.

$$\begin{aligned} &n_j = N_l, \quad \text{for } j = 6(i-1) + l, (l = 1, \ldots, 6), (i = 1, \ldots, NB) \\ &n_j = 0, \quad \text{for others.} \end{aligned} \tag{2}$$

Boundary condition of diffraction problem is the same as that in the case of single body. That is, multi-body system is regarded as fixed one body.

$$\frac{\partial \phi_{\mathrm{S}}}{\partial n} = -\frac{\partial \phi_{\mathrm{I}}}{\partial n}, \qquad \text{on } \sum_{k=1}^{\mathrm{NB}} S_k \tag{3}$$

Then the total potential (ϕ) is obtained by summation of incident wave potential (ϕ_{I}), scattering potential (ϕ_{s}) and radiation potentials (ϕ_j) assuming harmonic motions as follows:

$$\phi = A(\phi_{\mathrm{I}} + \phi_{\mathrm{s}}) + \sum_{j=1}^{6\times\mathrm{NB}} \eta_j \phi_j, \tag{4}$$

where, A is wave amplitude, η_j the complex amplitude of jth mode motion.

With help of Green's second identity, the velocity potentials are solutions of boundary integral equation. In this study, wave Green function (G) is used in the form of source and dipole.

$$c(\vec{x})\phi(\vec{x}) = -\sum_{j=1}^{\mathrm{NB}} \int_{S_j} \phi(\vec{\xi}) G_{\mathrm{n}}(\vec{x}, \vec{\xi})\, \mathrm{d}S + \sum_{j=1}^{\mathrm{NB}} \int_{S_j} \phi_{\mathrm{n}}(\vec{\xi}) G(\vec{x}, \vec{\xi})\, \mathrm{d}S \tag{5}$$

where, $c(\vec{x})$ is so called solid angle, NB the number of bodies, G the wave Green function and subscript n the normal derivative with respect to $\vec{\xi}$. S_j denotes mean wetted surface of the jth body.

The irregular frequencies are removed with additional distribution of dipole on the interior water plane (Hong, 1987). No special assumption was made for the free surface region between the vessels. Discretization of the integral equation is performed using bi-quadratic 9 node quadrilaterals and 6 node triangular elements. The hydrodynamic forces are calculated by integrating hydrodynamic pressure on each body surface (Pinkster, 1976). More details are given in Choi and Hong (2002).

2.2. Time-domain analysis

Time-domain equation of motion for multiple-body can be obtained by expanding the transient equation of motion of a single body (Cummins, 1962) using generalized mode concept just like as for frequency-domain analysis.

$$\begin{bmatrix} M_{11}+m_{11} & \cdots & m_{1N} \\ \vdots & \cdots & \vdots \\ m_{N1} & \cdots & M_{NN}+m_{NN} \end{bmatrix} \begin{Bmatrix} \ddot{\vec{x}}_1 \\ \vdots \\ \ddot{\vec{x}}_N \end{Bmatrix} + \begin{bmatrix} \int_0^t R_{11}(t-\tau)\,\mathrm{d}\tau & \cdots & \int_0^t R_{1N}(t-\tau)\,\mathrm{d}\tau \\ \vdots & \cdots & \vdots \\ \int_0^t R_{N1}(t-\tau)\,\mathrm{d}\tau & \cdots & \int_0^t R_{NN}(t-\tau)\,\mathrm{d}\tau \end{bmatrix} \begin{Bmatrix} \dot{\vec{x}}_1 \\ \vdots \\ \dot{\vec{x}}_N \end{Bmatrix} + \begin{bmatrix} C_{11} & \cdots & C_{1N} \\ \vdots & \cdots & \vdots \\ C_{N1} & \cdots & C_{NN} \end{bmatrix} \begin{Bmatrix} \vec{x}_1 \\ \vdots \\ \vec{x}_N \end{Bmatrix} = \begin{Bmatrix} \vec{F}_1 \\ \vdots \\ \vec{F}_N \end{Bmatrix} = \vec{f}(\vec{x}_1, \dot{\vec{x}}_1, \ldots, \vec{x}_N, \dot{\vec{x}}_N, t) \tag{6}$$

where, M denotes body mass matrix, m the adcded mass matrix at infinity frequency, R the retardation function(memory function) matrix, C the hydrostatic restoring coefficient matrix, F the external force vector and x the motion vector. Subscript denotes the mode number. External force vector F includes wave exciting force, drift force, current force, wind force and mooring force. Hamming method (Hornbeck, 1975) is used for the integration of equation of motion in time-domain, appropriate tapering function is applied for suppression of initial impact forcing.

3. Model tests

In order to verify numerical results on hydrodynamic interactions between multiple bodies, model tests were carried out at KRISO Ocean Engineering Basin.

Table 1
Main particulars of LNG FPSO, LNGC and shuttle tanker (full scale)

Item	Unit	LNG FPSO (full)	LNG carrier (ballast)	Shuttle (ballast)
Length, L_{pp}	m	448.23	266.0	297.4
Breadth, B	m	70.0	43.4	56.0
Draft (FP)	m	14.255	9.4	8.90
Draft (mid)	m	14.255	9.4	10.2
Draft (AP)	m	14.255	9.4	11.74
Displacement	m^3	411,861	78,591	127,386
LCG	m	+8.345	+2.633	+10.872
Gm	m	9.685	8.35	17.184
KG	m	22.436	12.084	12.768
$k_{yy}=k_{zz}$	m	$0.25L_{pp}$	$0.25L_{pp}$	$0.25L_{pp}$
k_{xx}	m	$0.37B$	$0.35B$	$0.35B$

The models considered are LNG FPSO, LNGC and a shuttle tanker moored side-by-side pattern. Distance between the side walls of each vessel was set to be 4 m in full scale, respectively. Main particulars of the vessels are listed in Table 1 and test arrangement is shown in Fig. 1. The FPSO model is moored by 4 wire-springs (2 wire-springs attached at fore and after most locations, respectively) as shown in Fig. 1. Two mooring models were used for LNGC: the one is spring model (wire-spring is attached to the fore and after part of the LNGC in longitudinal direction, uncoupled with the FPSO), the other is fender-spring model moored to the FPSO (coupled mooring, see Fig. 1). Independent spring model is applied for the shuttle tanker. The spring constant of the each line is set to be 1270 kN/m in full scale.

A set of regular waves between 0.25 and 1.2 rad/s in full scale is used for various heading angles, 270°, 240°, 180° and 150°. 2-parameter ITTC spectrum is used for representing irregular sea state 5($H_{1/3}=3.25$ m, $T_p=9$ s). 6 d.o.f motions of each vessel are measured with photo sensors (RODYM6D), relative waves at 3 locations (midship and $\pm 0.3L$ from the midship, portside) of LNG FPSO are measured by capacitance type probe. Strain gauge type accelerometers are used for measuring horizontal and vertical accelerations. Drift forces are measured using tension load cells at the end of spring wire moored to the ships. All the signals were sampled at 50 Hz in model scale. Zero-upcrossing method was used for analyzing the measured data, only the steady-state parts free from reflection of incident waves were chosen for extracting response functions in the regular wave tests. Test scene for 2-body case is shown in Fig. 2.

4. Results and discussions

4.1. Hydrodynamic interaction characteristics of side-by-side moored vessels

Hydrodynamic interaction between multiple bodies can be interpreted as sheltering effects and resonance due to trapped water between the bodies. Presence of adjacent bodies affects hydrodynamic forces such as added mass, damping and waves excitation both to a weather side body and lee side body. In diffraction problem, weather side body

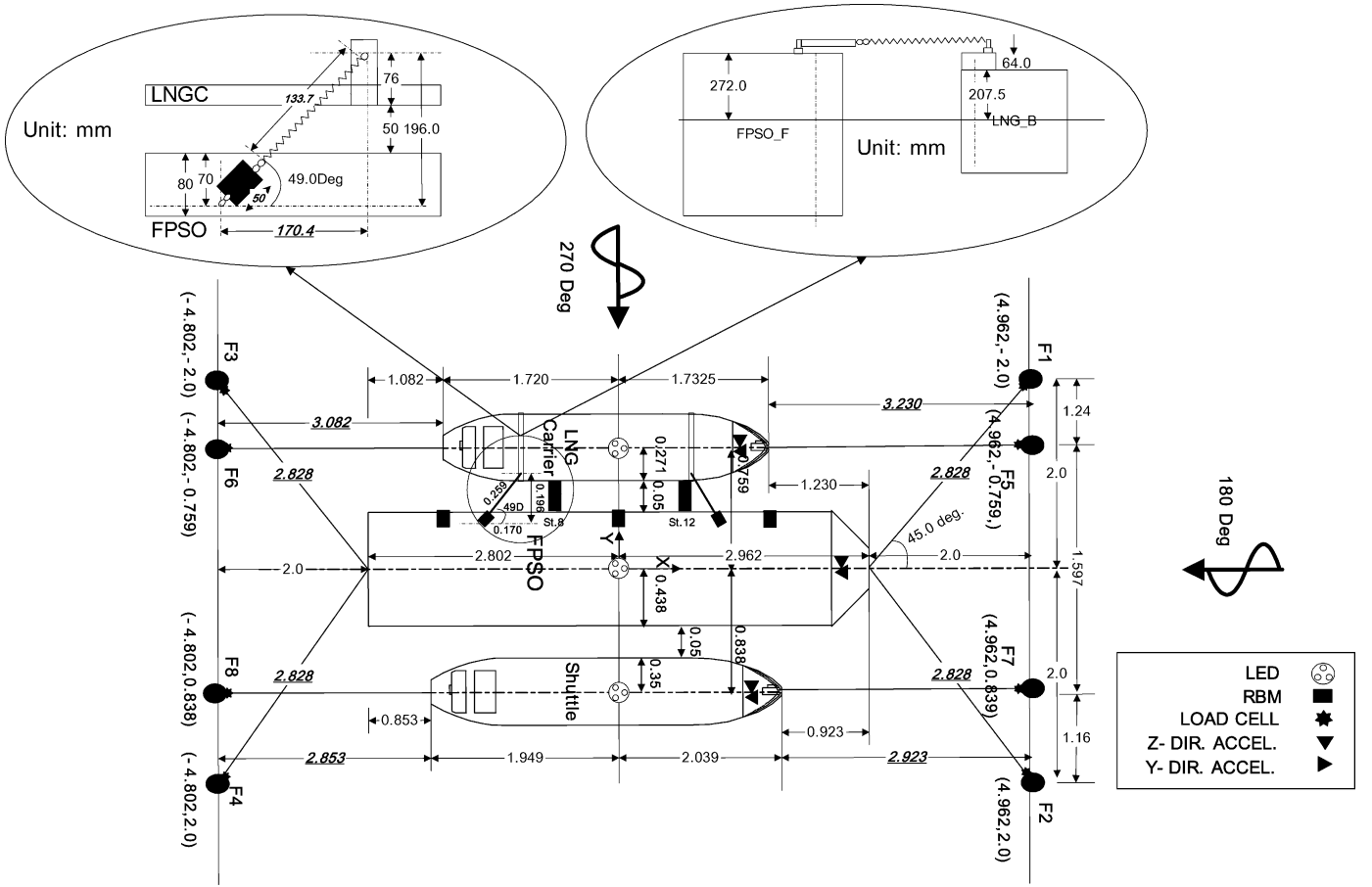

Fig. 1. Mooring configuration of side-by-side moored LNG FPSO, LNGC and shuttle tanker(unit is in meter in model scale unless definition is specified, scale ratio is 1/80).

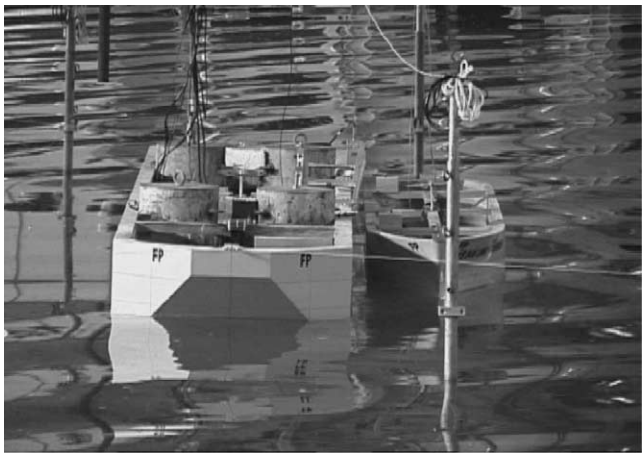

Fig. 2. Test scene for side-by-side moored LNG FPSO and LNGC.

acts as breakwater while a lee side body does as quay. In radiation problem one body acts as wave maker to the other body. Motion responses and drift forces are results of combined effects of radiation and diffraction. At frequencies of Helmholtz resonance where violent up and down motion of trapped water between two vessels occurs, strong interaction appears as sharp peaks in added mass and damping coefficients and exciting force curves.

Numerical results showing typical examples of hydrodynamic interactions between two side-by-side moored vessels are given in Figs. 3–7. Fig. 3 shows heave added mass and

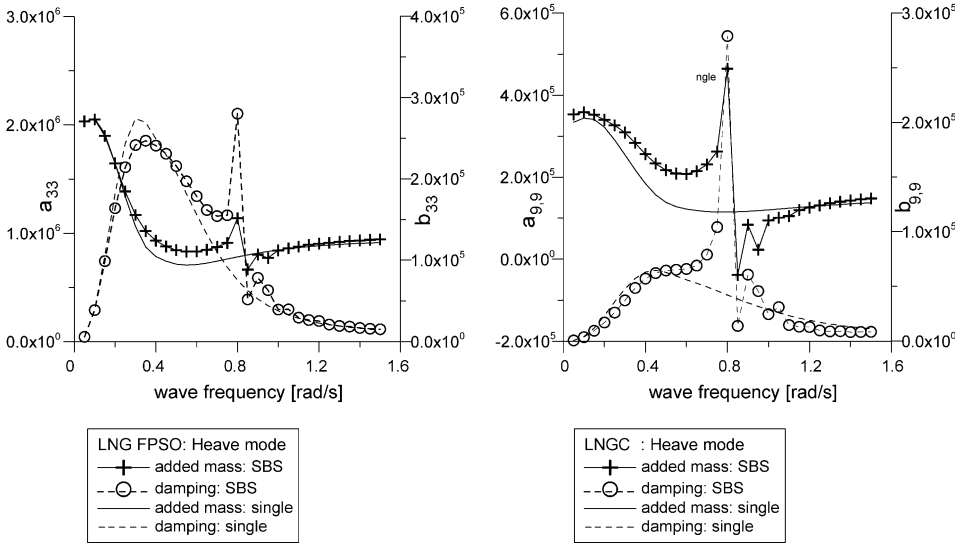

Fig. 3. Heave added mass and damping coefficients(LNG FPSO vs. LNGC).

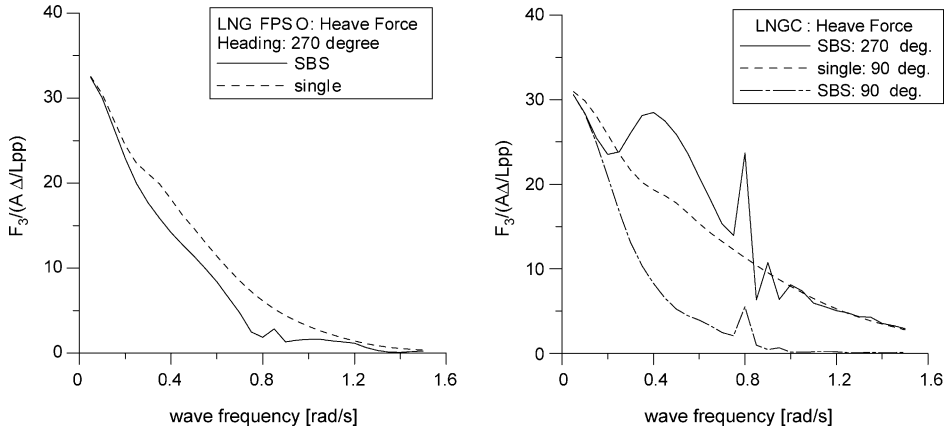

Fig. 4. Heave exciting forces on LNG FPSO and LNGC in beam sea.

damping coefficients of side-by-side moored LNG FPSO and LNGC. Significant interaction appears around 0.8 rad/s due to Helmholtz resonance of trapped water between two vessels. Heave exciting force shown in Fig. 4 represents typical sheltering effects due to neighboring body in beam sea. Such sheltering effect clearly results in heave response in Fig. 5, where the sheltering effect is more significant for LNGC than FPSO because of its size.

Interaction effects on wave drift forces are categorized as following three types: the first one is that nearby body contributes to increase of longitudinal drift force in head sea due to enhancement of blockage effect, the second one is the noticeable repulsive lateral drift forces produced near Helmholtz resonance frequency in head sea (Fig. 6), the last one is sheltering effects combined with the Helmholtz resonance effect (Fig. 7).

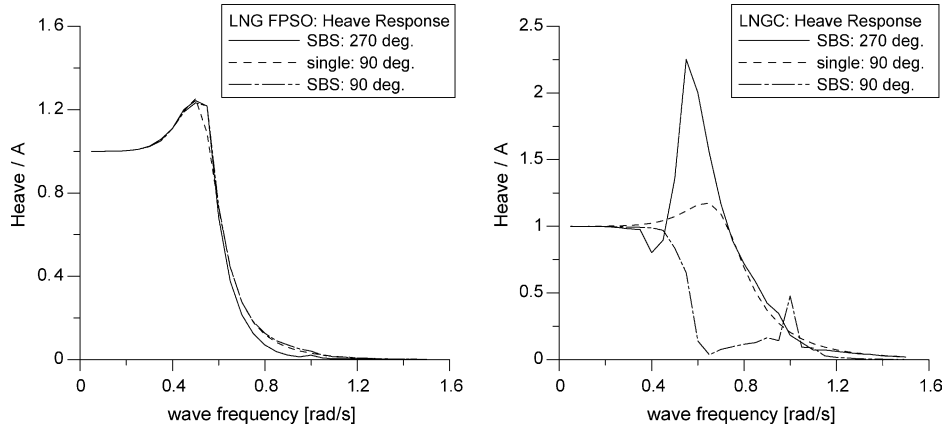

Fig. 5. Heave response of LNG FPSO and LNGC in beam sea.

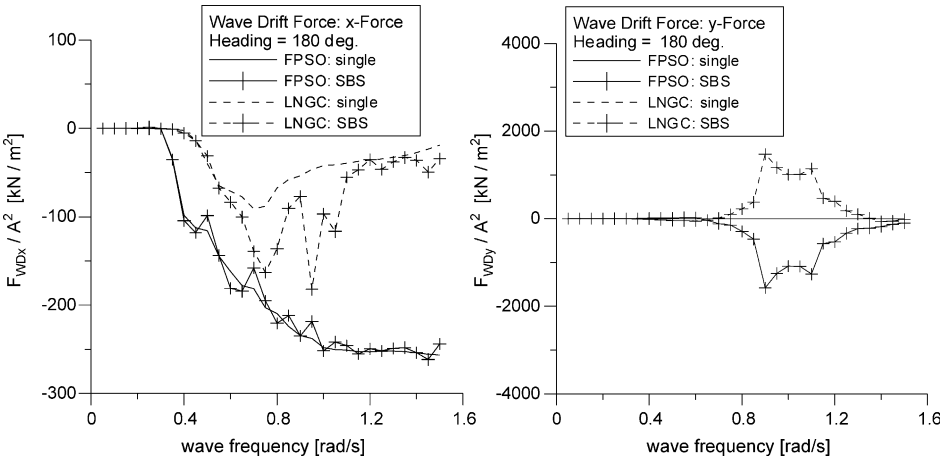

Fig. 6. Surge and sway drift forces on LNG FPSO and LNGC in head sea.

4.2. Comparison of model test results

Comparisons are made between the numerical results and model test results for the purpose of verification of the numerical results as well as understanding of multi-body hydrodynamic interactions. Global motion responses, local motions responses such as relative wave and acceleration, and drift forces are compared.

4.3.1. Motion response

Heave and pitch in head sea condition and heave and roll in beam sea condition of LNG FPSO and LNGC are compared in Figs. 8 and 9, respectively. Very good agreements are

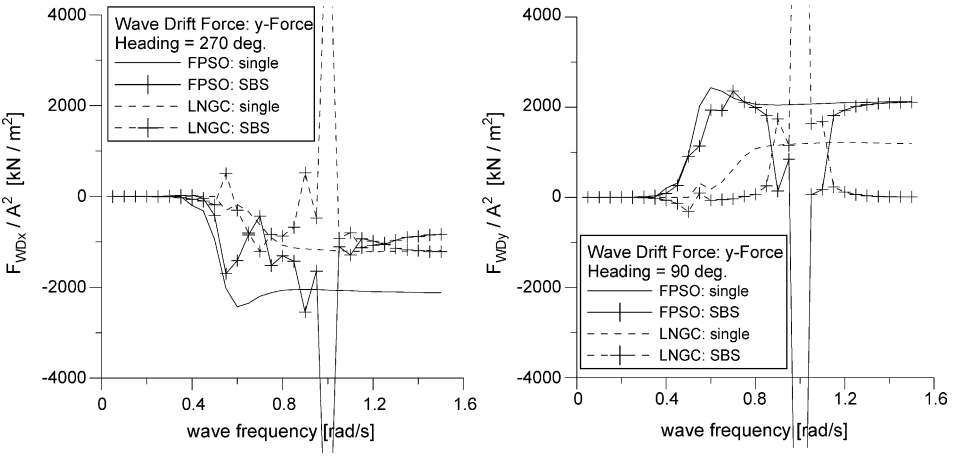

Fig. 7. Sway drift force on LNG FPSO and LNGC in beam sea.

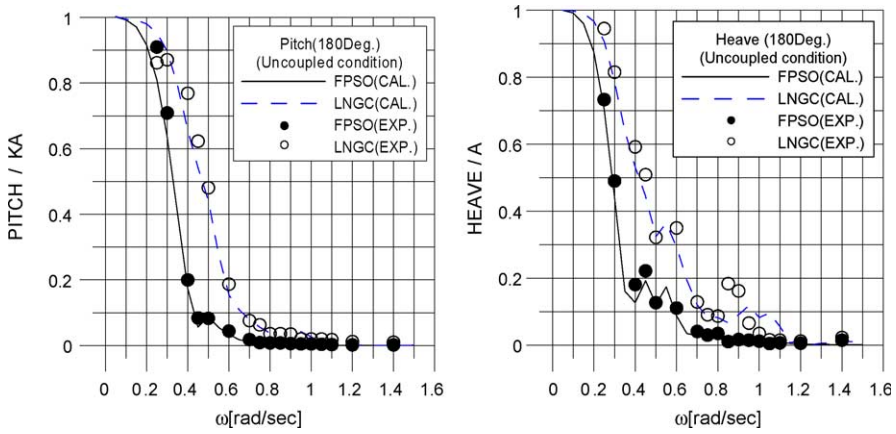

Fig. 8. Heave and pitch response of LNG FPSO and LNGC in head sea.

obtained both for head sea and beam sea conditions. No noticeable change of motion responses was observed for the coupled mooring case. From the comparisons of global motions, numerical estimation based on HOBEM seems to provide good motion predictions of side-by-side moored vessels with sufficient accuracy for engineering purpose.

4.3.2. Local motions

Comparison of local motions is another measure for investigating accuracy of the numerical calculations. Relative wave at mid ship of side-by-side moored LNG FPSO is compared for several heading conditions in Figs. 10 and 11. RBM in the figures denotes

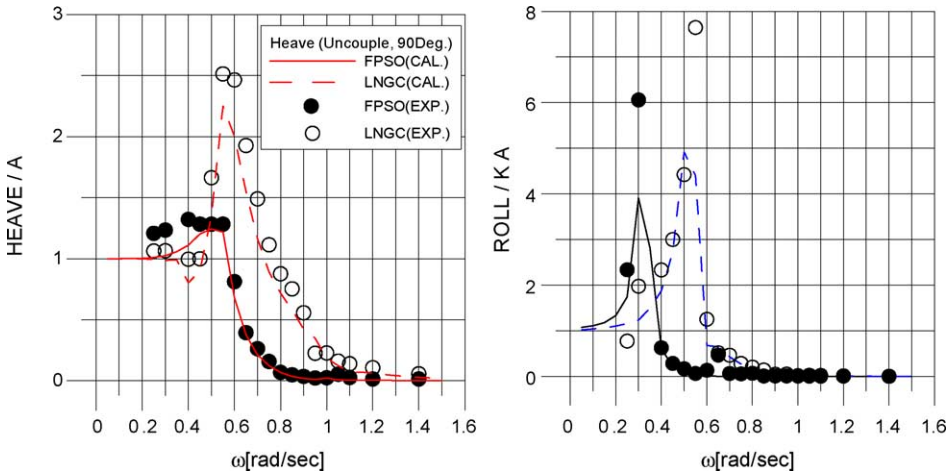

Fig. 9. Heave and roll response of LNG FPSO and LNGC in beam sea.

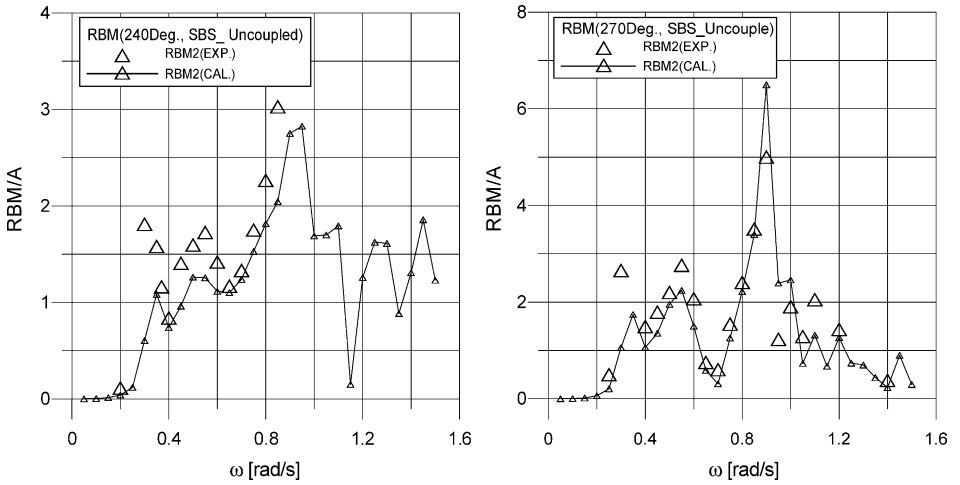

Fig. 10. Relative wave at mid ship of LNG FPSO(SBS mooring, 240 and 270 deg.).

relative bow motion as the same meaning of relative wave. Relative wave means the wave measured onboard. Generally good agreements in magnitude and trend are obtained for heading angles 150°, 240° and 270°. While noticeable discrepancy is observed for heading angles 180° as shown in Fig. 11, model tests results show that Helmholtz resonance is not so significant as in the calculations in head sea case. For other heading angles, however, Helmholtz resonance occurs clearly. This points out that arbitrary implementation of so called LID condition (Huijsmans et al., 2001) may mislead the numerical estimation. Relative wave is a major factor determining wave drift forces, this result implies that

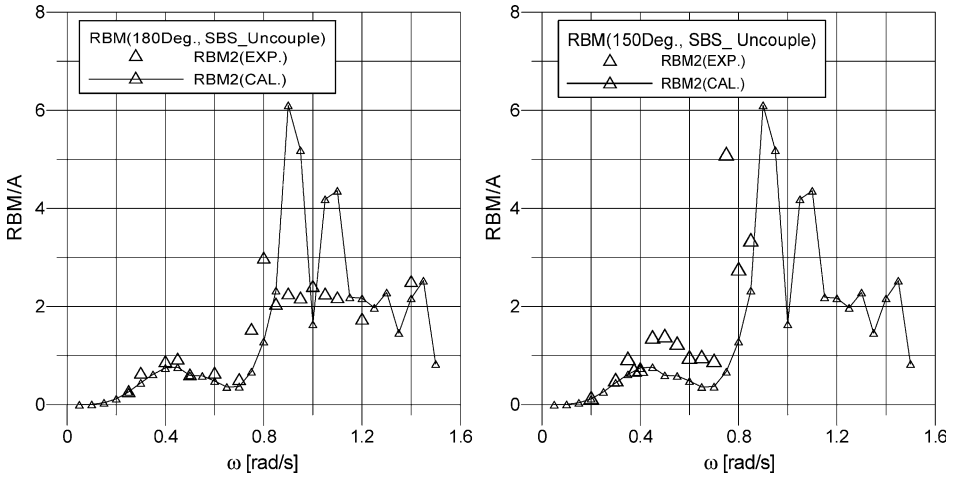

Fig. 11. Relative wave at mid ship of LNG FPSO(SBS mooring, 180 and 150 deg.).

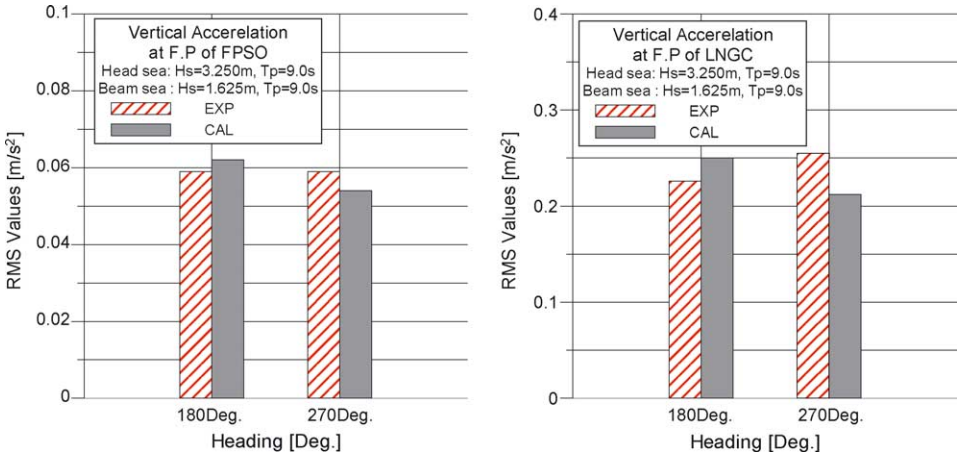

Fig. 12. RMS of vertical acceleration at FP of LNG FPSO and LNGC.

numerical calculation may overestimate lateral wave drift forces especially in head sea condition.

Fig. 12 shows vertical acceleration of LNG FPSO and LNGC at FP centerline in irregular head and beam sea conditions. Irregular sea states are $H_{1/3}=3.25$ m in head sea and $H_{1/3}=1.63$ m in beam sea, modal period is 9.0 s of ITTC spectrum. Fairly good agreements are obtained for the vertical accelerations both in irregular head and beam sea conditions. Slightly higher estimation in beam sea case might be due to reflection of incident waves.

4.3.3. Drift forces

For the verification of numerical accuracy up to second order, wave drift force is compared for side-by-side moored vessels (Hong et al., 2002).

Fig. 13 shows repulsive lateral wave drift forces on two tanker models in head sea condition. Good agreement is obtained for the case distance is 10 m, while noticeable discrepancy is observed near Helmholtz resonance frequency when the distance is 4 m. This result is qualitatively consistent with relative wave characteristics in head sea as shown in Fig. 11. Fig. 14 shows effect of distance on wave drift force in beam sea for the same models. For distance 10 m case, sheltering effect is dominant while strong interaction due to Helmholtz resonance is noticeable when the distance is 4 m. Except for narrow band of Helmholtz resonance frequency, quite good agreements are observed for lateral wave drift force in beam sea condition.

Table 2 shows comparison of drift forces obtained from regular and irregular wave tests. Generally good agreements are obtained between the two tests. It seems that coincidence in head sea case is better than the in beam sea case, irregular test results might be influenced by reflected waves.

Fig. 15 shows comparison of lateral wave drift force on side-by-side moored LNG FPSO and LNGC. The left one is for the case of the uncoupled mooring and the right one is

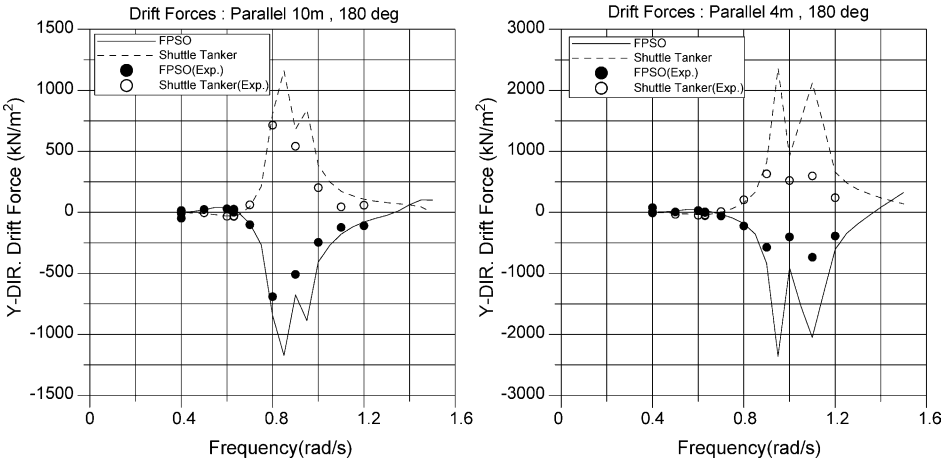

Fig. 13. Lateral wave drift force of side-by-side moored tankers in head sea (Hong et al., 2002).

for the coupled mooring case. Except for narrow frequency range of Helmholtz resonance frequency, quite good agreements between the experiments and the calculations are obtained for uncoupled mooring case. It seems that roll resonance is not so significant to accurate estimation of drift forces unlike Inoue and Islam (2001). In the coupled mooring case, the drift force was measured only for the LNG FPSO to which the LNGC is moored. The measured drift force is compared with the sum of drift forces on LNG FPSO and LNGC as shown in Fig. 15 (right), good agreement is also obtained for the coupled mooring case. This result supports the applicability of wave drift calculation based on

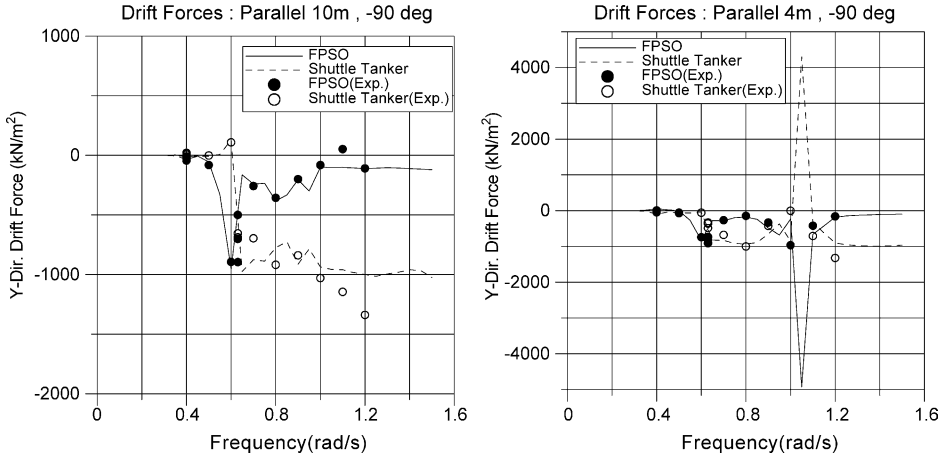

Fig. 14. Lateral wave drift force of side-by-side moored tankers in beam sea (Hong et al., 2002).

Table 2
Comparison of wave drift forces on side-by-side moored tankers in an irregular wave ($H_{1/3}$=3.0 m, ITTC 2-parapmeter spectrum, Hong et al., 2002)

Force heading distance		F_{WDx} (kN) 180 deg. S.B.S 4m	F_{Wdy} (kN) 180 deg. S.B.S. 4m	F_{Wdy} (kN) 90 deg. S.B.S. 10m	F_{WDy}, (kN) 90 deg. S.B.S. 4m
FPSO	Irregular	97.25	298.87	400.39	499.21
	Regular	97.16	253.13	299.15	448.80

HOBEM to designing mooring system of LNG FPSO to which LNGC is side-by-side moored.

Fig. 16 shows comparison of heave motion and wave drift force for side-by-side moored 3 vessels; LNG FPSO, LNGC and shuttle tanker. HOBEM numerical results show satisfactorily good agreements with experiments not only for global motion but also for wave drift force in 3-body coupled case.

4.3.4. Time-domain simulation

In time-domain analysis of multiple-body behavior, Buchner et al. (2001) addressed that use of fully coupled retardation function is prerequisite to consider hydrodynamic interaction accurately. In that case, the retardation function should be carefully evaluated due to occurrence of sharp peak near strong interaction frequency in damping coefficients. Sufficiently small frequency interval is required so as to resolve sharp peaks in the damping coefficients for calculating the retardation function accurately. At least two or three times of integration interval is needed for accurate implementation of convolution integral of time memory function comparing to single body case. It was also found that accurate estimation of added mass at infinity frequency is significant for ensuring stability of equation of motion.

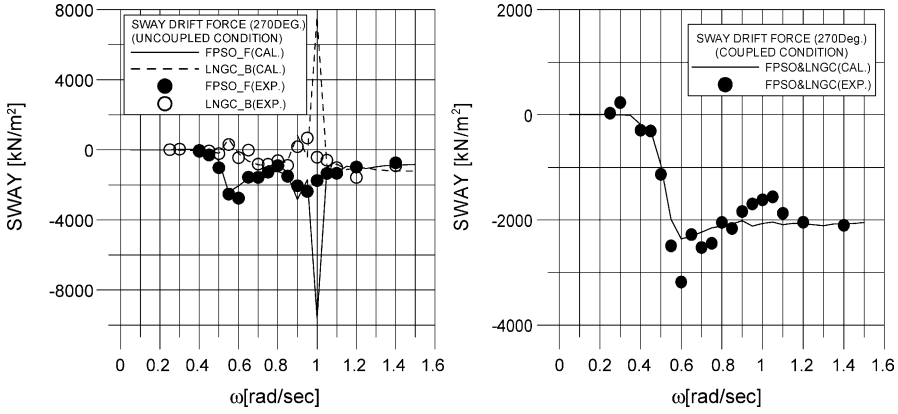

Fig. 15. Lateral wave drift force of side-by-side moored LNG FPSO & LNGC in beam sea.

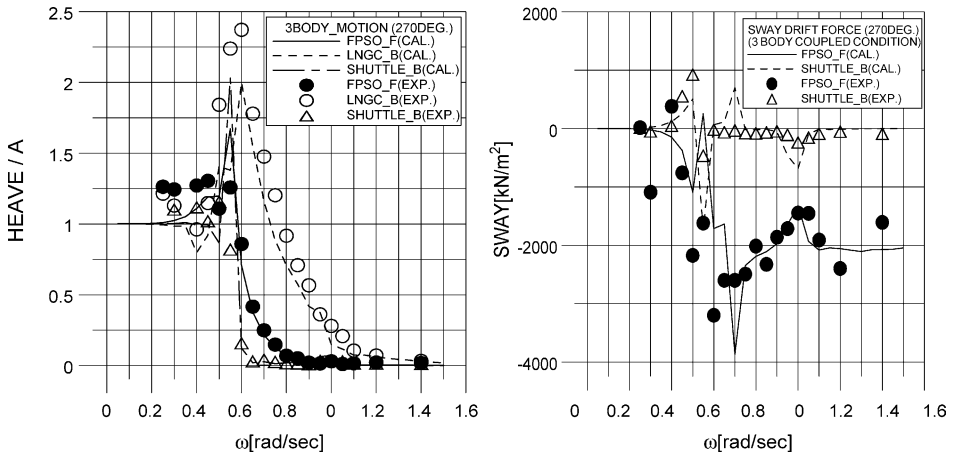

Fig. 16. Heave response and lateral drift force of side-by-side moored LNG FPSO, LNGC and shuttle tanker.

Fig. 17 shows comparison of motion spectra between time domain simulation and model tests for LNG FPSO and LNGC in irregular head sea($H_{1/3}=3.25$ m, $T_p=9.0$ s, ITTC spectrum). Mooring stiffness of LNG-FPSO and the LNGC are $k_{11}=k_{22}=k_{77}=$ 2540 kN/m, $k_{66}=3.26\times10^8$ kN m/rad. and $k_{12,12}=3.83\times10^7$ kN m/rad. Fully coupled retardation function is implemented and wave drift damping is considered for surge, sway and yaw following Clark et al. (1993). As seen in the figure, fairly good agreements are obtained for vertical mode motion (heave, roll and pitch) while noticeable discrepancies appear for surge, sway and yaw slow motions. No viscous effect is considered in the present study. As pointed out by Buchner et al. (2001), more studies on sophisticated sway–yaw coupled damping mechanisms are needed for realistic estimation of slow motion behavior of side-by-side moored vessels. Discrepancies in natural frequency of low frequency motions such as sway and yaw might be due to inaccurate numerical integration of convolution integral in spite of using fine frequency interval to calculate the retardation function.

5. Conclusions

Various aspects of hydrodynamic interactions of side-by-side moored multiple vessels are investigated by numerically and experimentally. From the numerical analysis using HOBEM and comparison with the experiments, the following conclusions are drawn.

1. Numerical results using HOBEM show satisfactorily good agreements with experiments for global and local motion response and wave drift force of side-by-side moored vessels in regular and irregular seas. Exception is observed only for a wave drift force in very narrow frequency region where strong interaction occurs due to Helmholtz resonance. The numerical results, however, predicts total wave drift force

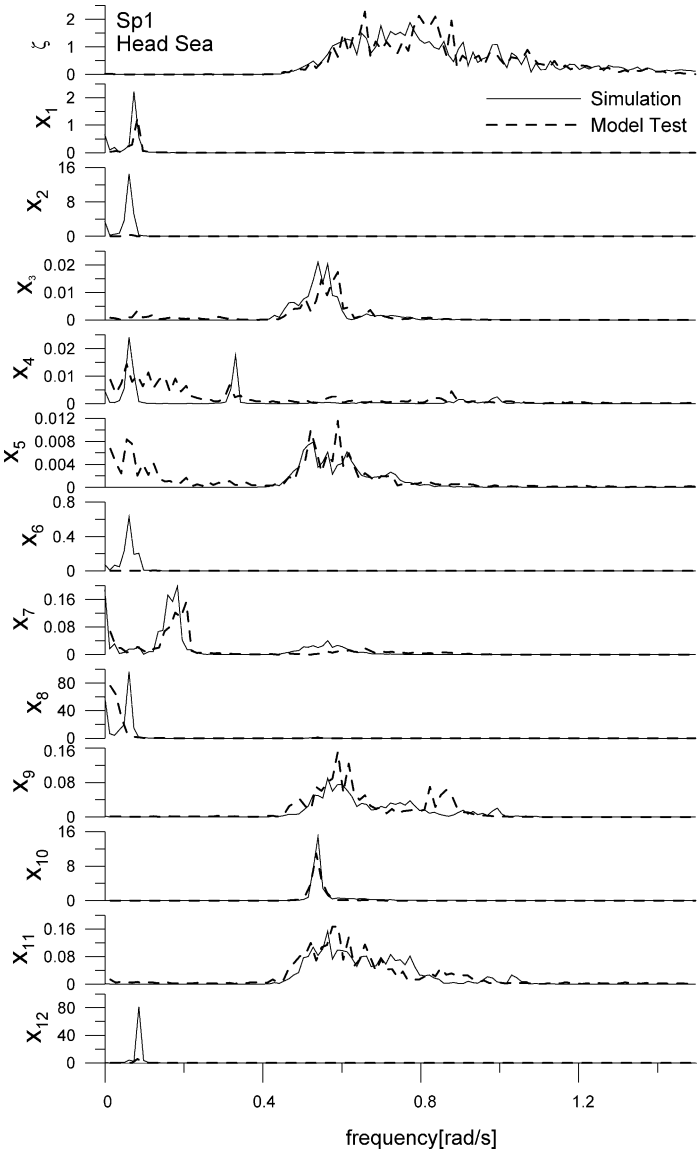

Fig. 17. Comparison of motion spectra of LNG FPSO and LNGC in head sea ($H_{1/3}=3.25$ m, $T_p=9.0$ s, units of spectral density are deg.^{2} seconds for $x_{4,5,6,10,11,12}$ and m^2 seconds for others.).

(sum of each vessels) even in Helmholtz resonance frequency, this fact supports accuracy and applicability of HOBEM to multi-body hydrodynamic interaction problem.

2. Wave drift force is not so significantly influenced by roll resonance motion for side-by-side moored vessels.

3. Helmholtz resonance phenomena are captured from the measured relative wave at mid ship of LNG FPSO to which LNGC side-by-side moored. The strength of interaction is reduced as heading angle changes from beam sea to head sea. The biggest discrepancy is observed at head sea condition comparing to numerical predictions.
4. Time domain simulation results provide practical estimation of vertical mode motions of side-by-side moored vessels as long as fully coupled retardation function is implemented, while more studies on coupled damping mechanism of planar motion is needed for improvement of slow motion estimation.

Acknowledgements

This work is a part of both the research programs, 'Enhancement of Design Engineering Technology for Ocean Development' supported by Korea Research Council of Public Science and Technology and 'Development of design technology of VLFS' funded by the Ministry of Maritime and Fisheries of Korea.

The authors are also grateful to partial support of Daewoo Shipbuilding and Marine Engineering Co., Ltd.

References

Buchner, B., Dijk, A., Wilde, J., 2001. Numerical multiple-body simulation of side-by-side mooring to an FPSO. Proceedings of 11th ISOPE, Stavanger 1, 343–353.

Clark, P.J., Malenica, S., Molin, B., 1993. An heurestic approach to wave drift damping. Applied Ocean Research 15, 53–55.

Choi, Y.R., Hong, S.Y., 2002. An analysis of hydrodynamic interaction of floating multi-body using higher-order boundary element method. Proceedings of 12th ISOPE, Kita-Kyushu 1, 303–308.

Fang, M.C., Kim, C.H., 1986. Hydrodynamically coupled motions of two ships advancing in oblique waves. Journal of Ship Research 30 (3), 159–171.

Fang, M.C., Chen, G.R., 2001. The relative motion and wave elevation between two floating structures in waves. Proceedings of 11th ISOPE, Stavanger 1, 361–368.

Fang, M.C., Chen, G.R., 2002. On three-dimensional solutions of drift forces and moments between two ships in waves. Journal of Ship Research 46 (4), 280–288.

Hong, D.C., 1987. On the improved green integral equation applied to the water-wave radiation-diffraction problem. Journal of Society of Naval Architects in Korea 24 (1), 1–8.

Hong, S.Y., Choi, Y.R., Kim, D.J., Kim, M.H., 1999. Responses of a barge-mounted platform in wave and current. Journal of Offshore and Polar Engineering, ISOPE 9 (4), 283–292.

Hong, S.Y., Kim, J.H., Kim, H.J., Choi, Y.R., 2002. Experimental study on behavior of tandem and side-by-side moored vessels. Proceedings of 12th ISOPE, Kita-Kyushu 3, 841–847.

Hornbeck, R.W., 1975. Numerical Methods. Quantum Publishers.

Huijsmans, R.H.M., Pinkster, J.A., de Wilde, J.J., 2001. Diffraction and radiation of waves around side-by-side moored vessels. Proceedings of 11th ISOPE, Stavanger 1, 406–412.

Inoue, Y., Islam, R., 2001. Effect of viscous roll damping on drift forces of multi-body floating system in waves. Proceedings of 11th ISOPE, Stavanger 1, 279–285.

Kodan, N., 1984. The motions of adjacent floating structures in oblique waves, Proceedings of Third· Offshore Mechanics and Arctic Engineering, vol. 1. OMAE, New Orleans pp. 206–213.

KRYPTON Electronic Engineering, 2001. RODYM DMM REALTIME MODULE Version 2.1, Belgium.

Lee, D.H., Choi, H.S., 1998. The motion behavior of shuttle tanker connected to a turret-moored FPSO. Proceedings of Third International Conference on Hydrodynamics 1998;, 173–178.

Liu, Y.H., Kim, C.H., Lu, X.S., 1990. Comparison of higher-order boundary element and constant panel methods for hydrodynamic loadings. Journal of Offshore and Polar Engineering, ISOPE 1 (1), 8–17.

Loken, A.E., 1981. Hydrodynamic interaction between several floating bodies of arbitrary form in Waves. Proceedings of International Symposium on Hydrodynamics in Ocean Engineering, NIT, Trondheim 2, 745–779.

Newman, J.N., 1977. Marine Hydrodynamics. MIT Press, Cambridge, MA.

Ohkusu, M., 1974. Ship motions in vicinity of a structure. Proceedings of International Conference on Behavior of Offshore Structure, NIT, Trondheim 1, 284–306.

Pinkster, J.A., 1976. Low frequency second order wave forces on vessels moored at sea. Proceedings of 11th Symposium on Naval Hydrodynamics 1976;, 603–615.

Van Oortmerssen, G., 1979. Hydrodynamic interaction between two structures of floating in waves. Proceedings of BOSS ‘79. Second International Conference on Behavior of Offshore Structures, London 1979;, 339–356.